SurFACTS in
Biomaterials

From the Editor

By Joe McGonigle, SurFACTS Executive Editor

The last issue came out as I was headed to BioInterface 2012 and I'm happy to report that the meeting was a tremendous success. I greatly enjoyed my first trip to Ireland where, for once, everyone I met was able to correctly pronounce my last name. The meeting provided a good chance to connect with members of the Surfaces in Biomaterials Foundation as well as a chance to meet many new European scientists working in the biomaterials field. For me, the conference provided a great introduction to plasma surface treatment, antimicrobial coatings and ultra-low fouling polymer coatings. BioInterface also showcased a broad review of the state-of-the-art in surface analysis, surface modification, biomaterials and drug delivery from both an industrial and academic perspective. Finally, I learned very important scientific details on the proper protocols to brew, pour and consume Guinness stout.

I'd like to thank all the contributors to this issue in *SurFACTS* and would like point out the excellent article submitted by Boston Scientific and the Characterization Facility at the University of Minnesota, which are both Surfaces in Biomaterials Foundation members. As a reminder, publishing in *SurFACTS* is a benefit for member companies and academic institutions. I'd also like to acknowledge the article by Niall Maloney from Trinity College Dublin, who won the award for best student poster at BioInterface 2012.

I hope all who attended enjoyed the meeting and I look forward to seeing everyone again in Minneapolis in the fall.

Inside this Issue

Strain-induced Crack Formations in PDMS/DXA Drug Collars

by Warner, J. A.*, Polkinghorne, J. C.**, Sarafolean, J.**, Meyer, S.**, Luo, B.*, Frethem, C.*, Haugstad, G.*, University of Minnesota (*) and Boston Scientific Corporation (**)

Abstract

Drug-eluting systems are currently used in cardiac leads in order to reduce inflammation and fibrosis at the lead-tissue interface. Drug release from these drug delivery systems can be modulated by the manufacturing processes used to create the drug systems and assemble them onto the cardiac lead. In this study, scanning electron microscopy (SEM), atomic force microscopy (AFM), and Raman microscopy are employed to explore the material characteristics of a polydimethylsiloxane-dexamethasone acetate (PDMS-DXA) drug collar used on cardiac leads when varying the strain during collar assembly on the lead.

A novel test fixture was created in order to investigate these drug collars under simulated stresses. Measurements of the collar while fitted to a rod revealed micro-cracks that are hypothesized to affect the drug release performance, resulting in increased drug elution. It was found that the strain that occurs during assembly of the collar onto the lead is a key factor in the formation of these micro-cracks. Results also suggest that cracks tend to form in areas of high drug particle density, and propagate between drug particles.

Introduction

When inserted into the endocardium for electrotherapy, cardiac leads may cause damage to the cardiac syncytium via inflammation and posterior fibrosis, resulting in increased threshold voltages[1, 2]. However, the addition of a drug component on the distal end of the lead has been shown to lessen the inflammation and significantly diminish the formation of a fibrous capsule surrounding the electrode, ultimately resulting in a reduction of the threshold voltage[3, 4]. This drug delivery system is typically composed of a two-phase system: for example, a continuous polydimethylsiloxane (PDMS) phase (a SiO2-reinforced matrix) and a dispersed phase consisting of the drug dexamethasone acetate (DXA)[5, 6].

The present work attempts to determine the effect that stretching (during assembly of a drug-containing component onto the lead) has on drug elution over time. The surface of the base of the drug collar is characterized by confocal Raman microscopy, atomic force microscopy (AFM), and scanning electron microscopy (SEM). These characterization tools may assist in understanding the mechanisms and pathways of drug elution for a drug collar in its realistic, stretched state, as it rests on the lead. Ultimately, developing knowledge of key factors that can influence drug elution time profiles, as well as the mechanisms of drug delivery, would be advantageous in guiding design of refined devices.

Materials and methods

Samples were created by either combining micronized dexamethasone acetate with a two-part platinum-catalyzed, silica (SiO2) reinforced PDMS elastomer to a 33 wt% drug loading followed by molding into drug collar components or molding the PDMS without drug incorporated into collar components. Each collar was assembled by stretching the component followed

by placement onto the rod feature of a test structure fabricated out of a polycarbonate material. The test structure, illustrated in Figure 1, was used to simulate placement onto a pacing lead and facilitate characterization of the drug collar in its stretched state.

Raman measurements were conducted on a WITec alpha 300R confocal Raman microscope (WITec Instrument Corp., Germany) equipped with a UHTS 300 spectrometer, a DV401 CCD detector and a piezo-driven, feedback-controlled scan stage that provides 4 nm lateral and 0.5 nm vertical positioning accuracy. A 100× Nikon air objective with a numeric aperture of 0.90 was used.

AFM was conducted with a Bruker Nanoscope V Multimode 8 (Santa Barbara, CA, USA), employing PeakForce QNM® (Quantitative Nanomechanical Mapping). The method provides simultaneous measurements of several characteristic sample metrics, which are herein referred to as height, tip-sample adhesive force, and "DMT Modulus" per the proprietary instrument software. Height refers to the Z scanner displacement to reach the PeakForce setpoint (quantified below), and thus to first approximation measures surface topography, but with possible higher-order effects due to differences of mechanical compliance (indentation) on rigid compared to soft surface locations. Tip-sample adhesive force is simply a measurement of the most negative deflection of the

cantilever due to attractive forces sensed during retraction.

The silicon tips employed (nominal radius of curvature 10 nm) were integrated with aluminum-backside-coated silicon cantilevers (rectangular, nominal spring constant 1.75 N/m, Mikromasch USA).

Results and Discussion

Two important aspects were revealed via SEM: drug particle aggregation and crack propagation. Figure 2a displays an SEM image of drug particles embedded in the PDMS broken up through cryo-sectioning. Unlike initial cryo-fracturing attempts, drug aggregates have been sectioned through, revealing sub-micrometer drug particle sizes. Figure 2b shows a large drug particle, broken into several pieces, resting in the PDMS. These semi-crystalline aggregates also appear to influence crack propagation in the PDMS, as both of these images showed cracks leading away from the larger drug aggregates, or larger drug particles.

Supporting evidence for drug elution through these microscopic cracks was provided via confocal Raman microscopy. Images were obtained by combining the individual DXA and PDMS spectra. Confocal Raman microscopy reveals the distributions of the DXA drug and PDMS polymer in an un-stretched sample and a stretched collar, as illustrated in Figure 3. A total of 2500 spectra collected at 5 spectra per μm (e.g. 5 pixels/μm) were used to produce these images. The green pixels denote the PDMS polymer, while the red pixels correspond to the interspersed DXA drug. Yellow regions are areas of DXA and PDMS
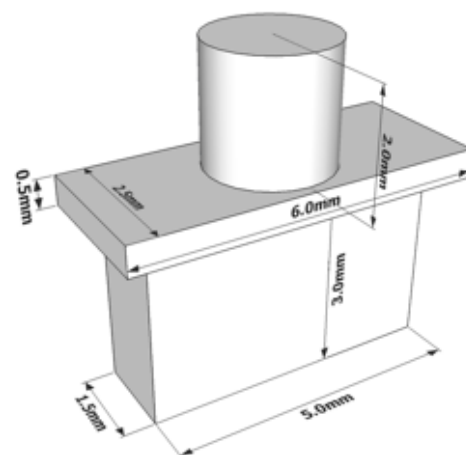
Figure 1. Test structure with rod feature used for analysis of drug collar in stretched state, simulating drug collar assembled on pacing lead. SEM and AFM imaging were performed on the top surface of the drug collar.

occupying the same pixel space. This is because the analysis volume (i.e., voxel) of each spectrum is ca. (0.30 × 0.30 × 0.60) μm, which sometimes contained both DXA and PDMS. Different color scales are used in these images. In general, bright red or green color indicates stronger signals of the corresponding component, and vice versa. The dark regions indicate weak Raman signals of both components.

The dark regions marked with the white arrows in Figure 3 have sizes substantially larger than the above-discussed dark spots. We attribute these dark regions as voids in the samples. Comparing to the un-stretched samples, more voids are present in the stretched sample (Figure 3 (d)) and most of them are located around the drug particles, consistent with the AFM and SEM results. One such void is detected in the depth profile (Figure 3 (c)). The formation of more voids upon stretching implies a weak polymer-drug interaction.

AFM measurements were also performed on drug-containing collars. Figure 4 displays representative images of the surface of the drug collar, where

Figure 2. SEM images of the surface of the drug collar following cryo-sectioning. (a) Demonstrates the cracks following drug particle locations. (b) Highlights a drug particle resting in the PDMS with cracks propagating away.

the stiffness measurements have been overlaid on top of the height images in order to provide sharper contrast. Locations of (i) PDMS, (ii) SiO2, and (iii) DXA are denoted in Figure 4a. Because single values change for the "DMT Modulus" due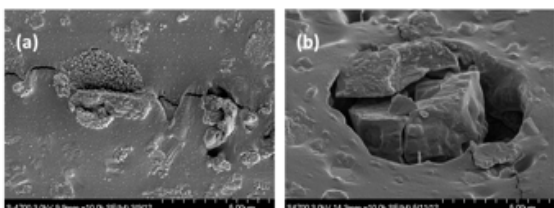 to cantilever changes and the aforementioned reservations of using this contact model, stiffness ratios would be more appropriate to state for PDMS, SiO2, and DXA, which
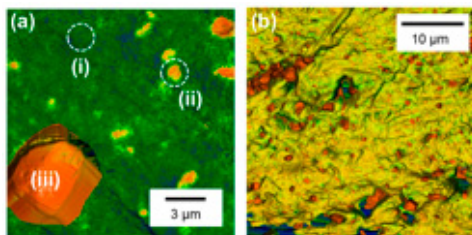
Figure 4. AFM stiffness contrast overlaid on 3D-rendered topography of the drug collar. Values of higher relative stiffness are brown/orange (DXA and SiO2), while those of lower stiffness (PDMS) are green/yellow. (a) Image identifying locations of (i) PDMS, (ii) SiO2, and (iii) DXA. (b) larger image.

are 1:13:42, respectively. Unless the DXA resides on the surface of the PDMS, however, the relative stiffness of the DXA may be reduced. Therefore, morphology and particle size are more easily used to differentiate DXA and SiO2.

In Figure 4b, the drug particles are clearly identified in orange, and appear to aggregate together in the upper left portion of the scan, inside a small crack. The voids, where the drug particles do not fully occupy the PDMS, are denoted by a green and blue coloring. This indicates a lack of contact between tip and sample due to the deep void the DXA resided in, reminiscent of the SEM image in Figure 2b.

Beyond differentiation of the three components based on stiffness, AFM measurements further provided insight into crack propagation in the collars. Figure 5 displays a 40 μm × 40 μm scan of

the drug collar with a crack propagating across the surface. Figure 5a and Figure 5b are the same scan, with height in (a) and adhesion in (b). Other scans revealed this same preponderance of drug along cracks, providing more evidence for crack propagation between drug particles.

Conclusion

SEM, confocal Raman microscopy, and AFM provided insight into the physical perturbation of drug collars as a result of stretching that can influence elution. SEM revealed crack propagation stems from drug particles. Raman confirmed that particles visualized in SEM were DXA drug, and also confirmed crack formation initiates at drug particles. Raman microscopy further reveals a possible additional component present, which was assumed to be silica filler, further explored by AFM. AFM confirmed the presence of these small particles in range of 10 – 300 nm, which is proposed to be the filler. AFM further demonstrated drug particle aggregation and allowed the differentiation of PDMS, DXA, and SiO2.

References

1. Sambelashvili AT, Nikolski VP, Efimov IR. Virtual electrode theory explains pacing threshold increase caused by cardiac tissue damage. American Journal of Physiology Heart and Circulatory Physiology 2003; 286:2183-2194.

2. Furman S, Hurzeler P, Parker B. Clinical thresholds of endocardial cardiac stimulation: A long-term study. The Journal of Surgical Research 1975; 19:149-155.

3. Mond HG, Stokes KB. The electrode-tissue interface: The revolutionary role of steroid elution. Pacing and Clinical Electrophysiology 1992; 15: 95-107.
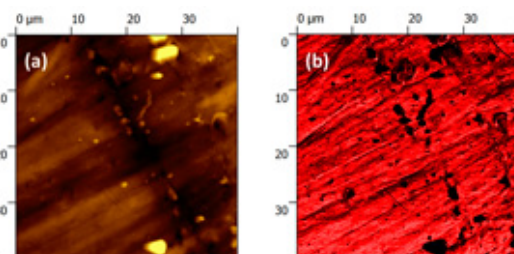
Figure 5. AFM images containing a crack in the surface of the PDMS/drug matrix. (a) Height. (b) Adhesion. Brighter corresponds to greater values of pull-off force.
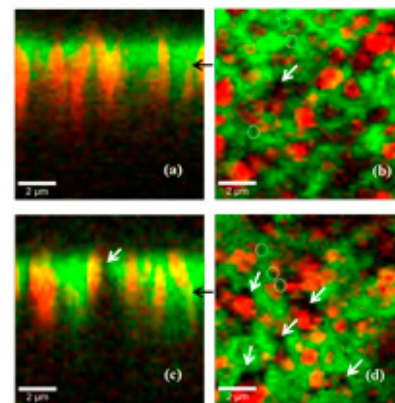
Figure 3. Raman images of the PDMS drug collar: (a) depth profile of the un-stretched sample – the sample surface is at 1.5 μm from the top edge, (b) lateral cross section of the un-stretched sample obtained at the depth marked with a back arrow in (a), (c) depth profile of stretched collar – the sample surface is at 1.5 μm from the top edge, (d) lateral cross section of the stretched collar obtained at the depth marked with a black arrow in (c).

4. Santini M, De Seta F. Stimulation TIMSGoLO: Do steroid-eluting electrodes really have better performance than other state-of-the-art designs? Pacing and Clinical Electrophysiology 1993; 16:722-728.

5. Golomb G, Fisher P, Rahamim E. The relationship between drug release rate, particle size, and swelling of silicone matrices. Journal of Controlled Release 1990; 12:121-132.

6. Simmons A, Padsalgikar AD, Ferris ML, Poole-Warren LA. Biostability and biological performance of a pdms-based polyurethane for controlled drug release. Biomaterials 2008; 29:2987-2995.

7. Soulas DN, Sanopoulou M, Papadokostaki KG. Comparative study of the release kinetics of osmotically active solutes from hydrophobic elastomeric matrices combined with the characterization of the depleted matrices. Journal of Applied Polymer Science 2009; 113:936-949.

8. Riggs PD, Kinchesh P, Braden M, Patel MP. Nuclear magnetic imaging of an osmotic water uptake and delivery process. Biomaterials 2001; 22:419-427.

9. Di Colo G. Controlled drug release from implantable matrices based on hydrophobic polymers. Biomaterials 1992; 13:850-856.

10. Lotters JC, Olthuis W, Veltink PH, Bergveld P. The mechanical properties of the rubber elastic polymer polydimethylsiloxane for sensor applications. Journal of Micromechanical Engineering 1997; 7:145-147.

11. Johnson KL, Kendall K, Roberts AD. Surface energy and the contact of elastic solids. Proceedings of the Royal Society of London 1971; 324:301-313.

12. Grierson DS, Flater EE, Carpick RW. Accounting for the jkr-dmt transition in adhesion and friction measurements with atomic force microscopy. Journal of Adhesion Science and Technology 2005; 19:291-311.

13. Haugstad G. Atomic force microscopy: understanding basic modes and advanced applications. 1st ed., Wiley 2012.

14. Israelachvili JN. Intermolecular and surface forces. Academic Press 2010.

15. Li L, Mangipudi V, Tirrell M, Pocius A. Fundamentals of tribology and bridging the gap between the macro- and micro/ nanoscales. Klewer Academic Publications 2001,

Hydrogel Functionalised Cantilevers for Microorganism Growth Detection

By Niall Maloney, Trinity College Dublin, BioInterface 2012 Student Poster Award Winner

Detection of viable microorganism growth is of great importance in several areas of microbiology. Microbial infection through contamination still poses a threat in areas such as the pharmaceutical, cosmetic and food industries. For this reason quality control is essential; tests are carried out to ensure microorganism contamination does not occur and that preservatives are functional. In clinical settings there has been an increase in the number of patients presenting with infections which show antibiotic resistance. Methods to date rely on conventional culturing and counting methods which are labour, material and time intensive. Currently in hospital laboratories, advanced tests performed to make an empirically established decision for treatment of infection require approximately 4 days. Thus, a rapid and reliable growth detection mechanism would be highly advantageous.

High mass sensitivity[1] accompanied by an increased use as biosensor in recent years indicates that cantilever arrays have the potential to be used for fast microorganism growth detection. When operated in dynamic mode the cantilever acts as a "mass balance" by actuation at its resonance frequency. Mass loading on the cantilever results in a decrease in resonance frequency. Arrays consisting of eight individual cantilever bars, each having a length, width and thickness of 500 μm, 100 μm and 0.5-7 μm respectively are used in our studies. A pitch of 250 μm separates each cantilever. The use of multiple sensors on one array allows for several tests to be performed in parallel (i.e. susceptibility testing using different concentrations of antibiotics) while also allowing for the use of in-situ reference sensors, which eliminate false positive or negative signals.

Readout of the biological sensor uses the laser beam deflection method which is widely utilized in the field of atomic force microscopy. A schematic of the device is shown in Figure 1. A focused laser spot is deflected off the cantilever surface onto a position sensitive detector (PSD) which is
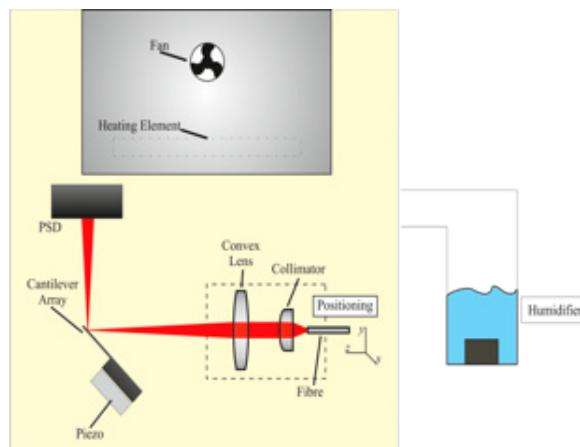

Figure 1. Schematic of cantilever sensor array device. A focused laser spot is deflected off the sensor's surface onto a PSD which is used to track the resonance frequency of the cantilevers in the array. Two automated translation stages are used to move the laser spot from sensor to sensor and along each sensor in the array. A piezo ceramic is used to actuate the cantilevers at their resonance frequencies. The device is fully automated via LabVIEW. The device is housed in a custom designed environmental chamber.

employed to track the resonance frequency of the cantilevers in the array. Two automated translation stages are used to move the laser spot from sensor to sensor and along each sensor in the array. The cantilevers are actuated at their resonance frequencies by a piezo ceramic actuation stage. The device is fully automated via a LabVIEW software interface, which allows the resonance frequencies of the sensors in the array to be recorded in a time multiplexed fashion. Microorganism growth is dependent on the provision of suitable nutrition, water and temperature (30-37 °C). Water, via a humid environment (> 94 %), and temperature are provided by the custom designed environmental chamber in which the device is housed. This allows accurate control of relative humidity (RH) and temperature levels
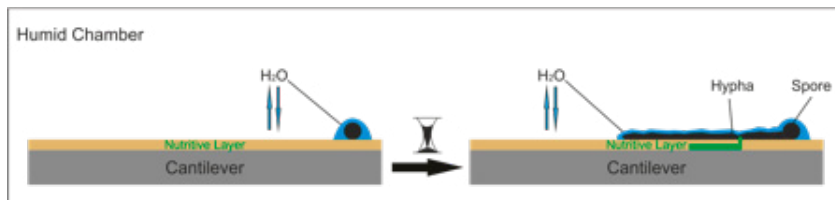

Figure 2. Mechanism for growth detection. A cantilever inoculated with an Aspergillus spore is in equilibrium with its surrounding environment. As time passes growth via hypha filaments occurs which results in an uptake of water on the cantilever's surface.

to within ±0.2 % and ±0.1°C respectively, which is essential for accurate growth detection measurements.

In preparation for growth detection measurements, the cantilevers are first cleaned using oxygen plasma. An epoxy-terminated silane monolayer is used to ensure covalent anchorage of thin agarose hydrogel layers on the cantilever surfaces. Functionalization of the cantilevers with agarose is achieved using dimension matched heated glass capillary tubes[2]. In order to form a nutritive layer on the cantilever surface the thin agarose hydrogel, which acts as a reservoir, is saturated with nutritional broth. Deposition of microbes on the cantilever can be performed using one of the following techniques; (i) ink jet printing[3], (ii) micro needle (for fine positioning of individual microbes), or (iii) capillary functionalization. While in the device chamber, water exchange between the nutritive layer and the surrounding environment is in equilibrium. As nutrition is already on the surface of the cantilever, any mass uptake is due to adsorption of water caused by microorganism growth (Figure 2).

Using this hydrogel functionalised sensor the detection of Aspergillus niger growth (Figure 3)[4], within 5 hours, and Escherichia coli growth[5], within 1 hour, has been reported by means of a previous iteration of the device. Utilizing the current device, as described in this article, tests have been performed which illustrate the susceptibility of Aspergillus spores to different concentrations of fluconazole. Results were obtained significantly faster than when conventional methods are used. The micron precise movement of the laser spot along the cantilever enables the readout of higher modes of vibration and thus increases the sensitivity[6] of the biological sensor. The positional effect of mass uptake on the cantilever when operated at higher resonance modes[7]
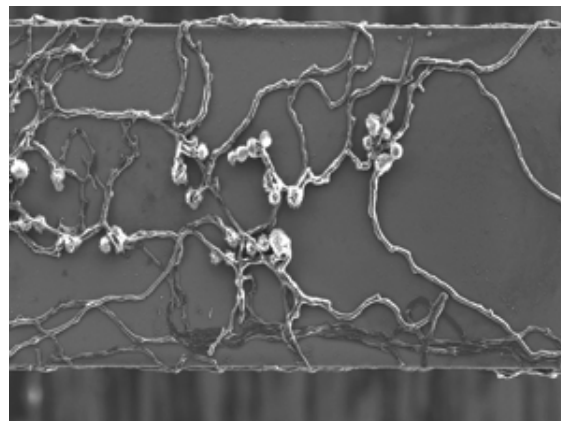

Figure 3. Scanning electron microscope image of Aspergillus niger hyphal growth on a cantilever. The thickness of the hyphae is of the same order of magnitude as the cantilever thickness (7 μm). Scale bar shown is 10 μm.

allows us to determine the rate of growth of Aspergillus hypha along the cantilever surface providing information on single cell mechanics. Further development of this device, by replacement of the current optical read-out by a piezo-resistive biosensor, will provide a user friendly handheld platform suitable for fast microorganism growth detection which will be applicable in several fields of microbiology.

References

1. M. Li, H.X. Tang, M.L. Roukes, Ultra-sensitive NEMS-based cantilevers for sensing, scanned probe and very high-frequency applications, Nature Nanotechnology, 2 (2007) 114-120.
2. H.P. Lang, M. Hegner, C. Gerber, Cantilever array sensors, Materials Today, 8 (2005) 30-36.
3. G. Lukacs, N. Maloney, M. Hegner, Ink-Jet Printing: Perfect Tool for Cantilever Array Sensor Preparation for Microbial Growth Detection, Journal of Sensors, 2012 (2012) 7.
4. N. Maloney, G. Lukacs, N. Nugaeva, W. Grange, J.P. Ramseyer, J. Jensen, M. Hegner, Fibre Optic Readout of Microcantilever Arrays for Fast Microorganism Growth Detection, Journal of Sensors, 2012 (2012).
5. K.Y. Gfeller, N. Nugaeva, M. Hegner, Micromechanical oscillators as rapid biosensor for the detection of active growth of Escherichia coli, Biosensors and Bioelectronics, 21 (2005) 528-533.
6. G. Murali Krishna, et al., Higher modes of vibration increase mass sensitivity in nanomechanical microcantilevers, Nanotechnology, 18 (2007) 445502.
7. D. Ramos, J. Tamayo, J. Mertens, M. Calleja, L.G. Villanueva, A. Zaballos, Detection of bacteria based on the thermomechanical noise of a nanomechanical resonator: origin of the response and detection limits, Nanotechnology, 19 (2008) 035503.

16. Silberzan P, Perutz S, Kramer EJ. Study of the self-adhesion hysteresis of a siloxane elastomer using the jkr method. Langmuir 1994; 10:2466-2470.

17. Chibowski E, Perea-Carpio R. Problems of contact angle and solid surface free energy determination. Advances in Colloid Interface Science 2002; 98:245-264.

18. Gonzalez-Martin ML, Janczuk B, Labajos-Broncano L, Bruque JM, Gonzalez-Garcia CM. Analysis of the silica surface free energy by the imbibition technique. Journal of Colloid Interface Science 2001; 240:467-472.

19. Pittenger B, Erina N, Su C. Quantitative mechanical property mapping at the nanoscale with peakforce qnm. Online. Available from URL: http://www.bruker-axs.com/ uploads/tx_linkselectorforpdfpool/Quantitative_Mechanical_ Property_Mapping_at_the_Nanoscale_with_PeakForce-QNM_AFM_AN128.pdf, Veeco Application Note, (2010).

20. Neas D, Klapetek P. Gwyddion: An open-source software for spm data analysis. Central European Journal of Physics 2012; 10:181-188.

21. Gotsmann B, Seidel C, Anczykowski B, Fuchs H. Conservative and dissipative tip-sample interaction forces probed with dynamic afm. Physical Review B 1999; 60:51

Designing Mechano-Responsive Materials with Elastomeric Properties for Biomedical Applications

By Xiaowei Yang, Longxi Xiao and Xinqiao Jia
Department of Materials Science and Engineering, University of Delaware

Synthetic polymers have been widely explored for use as tissue engineering scaffolds or smart medical devices.[1] The development of intelligent biomaterials that closely mimic the structural organizations and multi-scale responsiveness of the natural extracellular matrices (ECM) has become critically important in biomedical engineering.[2] Given the fact that most tissues in the body are subjected to mechanical stimuli, and cells within the tissue have sophisticated machinery that actively responds to the mechanical force, it is critical that this form of signaling be considered in the design of polymeric biomaterials.[3] An inevitable consequence of mechano-responsiveness is the tunability of materials' properties in response to the applied forces. In this article, we summarize our effort in designing synthetic biomaterials that are mechano-responsive. We emphasize the importance of incorporating mechano-responsive elements in synthetic matrices so that the materials' properties and the cellular functions can be dynamically controlled by physiologically relevant mechanical stimuli.

Figure 1. Chemical structures of ECT-AC (1)[5], [PEG-AK2]$_n$ (2a)[7] and [PEG-AK2(RGD)]$_n$ (2b)[8]

Poly(ε-caprolactone) (PCL)-based elastomers. Elastomers can undergo large and reversible deformations at relatively low stresses via force-induced alteration of polymer conformation from random coils to extended chains.[4] Therefore, elastomers are naturally mechano-responsive. We have synthesized and characterized PCL-based copolymers with flexible backbone and crosslinkable side chains. Specifically, ring opening polymerization of ε-caprolactone (CL) and 1,4,8-trioxaspiro-[4,6]-9-undecanone (TSU) using α-methoxy, ω-hydroxyl poly(ethylene glycol)

(mPEG) as the initiator afforded a copolymer (ECT-CK) with randomly distributed cyclic ketals in the hydrophobic block. Quantitative side chain deacetalization revealed the reactive ketone moieties, through which acrylate groups were conjugated via an oxime reaction. UV-initiated radical polymerization of acrylated copolymer (ECT-AC, 1, Fig. 1) in dichloromethane resulted in a crosslinked network (xECT-AC) containing stiff crystalline lamellae dispersed in a softer amorphous interstitial. Macroscopic and nanoscale mechanical characterizations showed a significant decrease in Young's modulus when the bulky cyclic ketals were incorporated. While ECT-CK undergoes a plastic deformation with a distinct yield point and a cold drawing region, xECT-AC exhibited a compliant, elastomeric deformation with a Young's modulus of 0.5 MPa at ~37 °C. When properly processed, the crosslinked network exhibited shape memory behaviors with shape fixity and shape recovery values close to 1 and a shape recovery time of ~4 s at 37°C.[5] The crosslinkable polyester copolymers can be potentially used as tissue engineering scaffolds or injectable medical devices.

Elastin mimetic hybrid copolymers. Elastin is abundant in mechanically active soft tissues. It is composed largely of two types of short segments that alternate along the polypeptide chain: highly flexible hydrophobic segments, with many transient structures that can easily change their conformation when stretched; and alanine- and lysine-rich α-helical segments that form covalent cross-links between adjacent molecules.[6] We have successfully synthesized elastin mimetic hybrid polymers (EMHPs) employing copper (I)-catalyzed alkyne-azide cycloaddition (CuAAC) reaction between telechelic, azide-terminated PEG and alkyne-functionalized peptide with a sequence of (AKAAAKA)$_2$ (AK2) that is abundant in the crosslinking region of the natural elastin.[7, 8] The resulting multiblock copolymers, [PEG-AK2]$_n$ (2a, Fig 1) have an estimated molecular weight of 34 kDa and are cytocompatible to the cultured cells. Covalent crosslinking of 2a through the lysine amines in peptide segments gave rise to elastomeric hydrogels with mechanical properties comparable to those
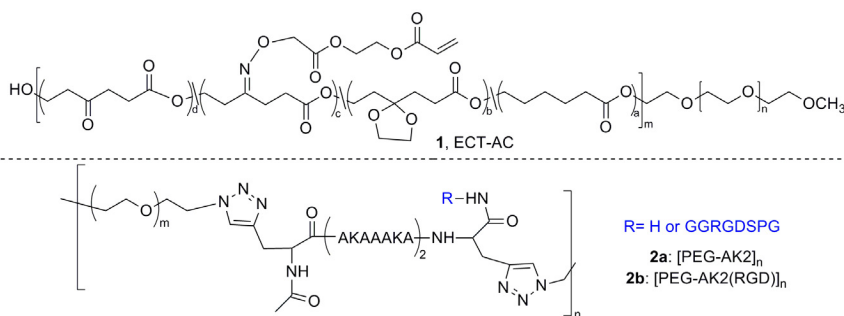
of the natural elastin.[7] To foster integrin-mediated cell adhesion, RGD-containing peptide with a sequence of X(AKAAAKA)$_2$XGGRGDSP was used in place of X-AK2-X (X=propargylglycine) for EMHP synthesis. The resultant copolymer, [PEG-AK2(RGD)]$_n$ (2b, Fig 1), when covalently crosslinked, facilitates integrin-mediated attachment and proliferation of neonatal foreskin fibroblasts.[8] These mechanically responsive materials can be fabricated into porous scaffolds for the engineering of mechanically active tissues, such as the vocal fold, tendons and cardiovascular systems.

Mechano-responsive hydrogels. Mechano-responsive structural motifs are abundant in nature. Through the coordinated conformational changes over a range of mechanical forces, these motifs can ultimately produce changes at the biochemical level to effectively direct cellular behaviors.[9-11] We have created a new type of hydrogel material using self-assembled block copolymer micelles (BCMs) as the dynamic building blocks combined with microscopic crosslinkers.[12, 13] Block copolymer micelles were assembled from amphiphilic block copolymer of poly(n-butyl acrylate) (PnBA) and acrylate-modified poly(acrylic acid) (PAA) (3, Fig 2). Radical polymerization of acrylamide in the presence of micellar crosslinkers gave rise to elastomeric hydrogels (BCM-PAAm gels, Fig 2) whose mechanical properties can be tuned by varying the BCM composition. Transmission electron microscopy imaging revealed that the relaxed BCM-PAAm gels contain perfectly spherical particles with an average diameter of 30±3 nm. When BCM-PAAm gels were stretched to 60% and 200% strain, the spherical micelles became ellipsoidal with the long axis parallel to the stretch direction, having an aspect ratio of 1.26 ±0.13 and 1.53 ±0.23, respectively. TEM characterization of control gels devoid of BCMs showed a featureless background stain at 0 and 60% strain. A model hydrophobic drug, pyrene, loaded into the core of the BCMs prior to the formation of BCM-PAAm gels, was dynamically released in response to externally applied mechanical forces, through force-induced reversible micelle deformation and the penetration of water molecules into the micelle core, leading to the weakening of hydrophobic association between pyrene and the micelle core.[13] If pyrene is replaced by biologically active molecules, mechanical forces can be readily converted into biochemical cues to facilitate tissue repair and regeneration.

References

1. Langer, R.; Tirrell, D. A. Nature 2004, 428, (6982), 487-492.

2. Lutolf, M. P.; Hubbell, J. A. Nature Biotechnology 2005, 23, (1), 47-55.

3. Tong, Z.; Jia, X. MRS Commun 2012, 2, 31-39.

4. Lal, J.; Mark, J. E., Advances in elastomers and rubber elasticity. Springer: 1987.

5. Yang, X.; Cui, C.; Tong, Z.; Sabanayagam, C. R.; Jia, X. Biomacromolecules 2012, submitted.

6. Debelle, L.; Tamburro, A. M. Int. J. Biochem. Cell Biol. 1999, 31, 261-272.

7. Grieshaber, S. E.; Farran, A. J. E.; Lin-Gibson, S.; Kiick, K. L.; Jia, X. Macromolecules 2009, 42, (7), 2532-2541.

8. Grieshaber, S. E.; Farran, A. J.; Bai, S.; Kiick, K. L.; Jia, X. Biomacromolecules 2012, 13, (6), 1774-86.

9. Tskhovrebova, L.; Trinick, J.; Sleep, J. A.; Simmons, R. M. Nature 1997, 387, (6630), 308-312.

10. Fantner, G. E.; Hassenkam, T.; Kindt, J. H.; Weaver, J. C.; Birkedal, H.; Pechenik, L.; Cutroni, J. A.; Cidade, G. A. G.; Stucky, G.; Morse, D. E.; Hansma, P. K. Nat. Mater. 2005, 4, 612-616.

11. Vogel, V.; Sheetz, M. Nat. Rev. Mol. Cell Biol. 2006, 7, 265-275.

12. Xiao, L. X.; Liu, C.; Zhu, J. H.; Pochan, D. J.; Jia, X. Q. Soft Matter 2010, 6, (21), 5293-5297.

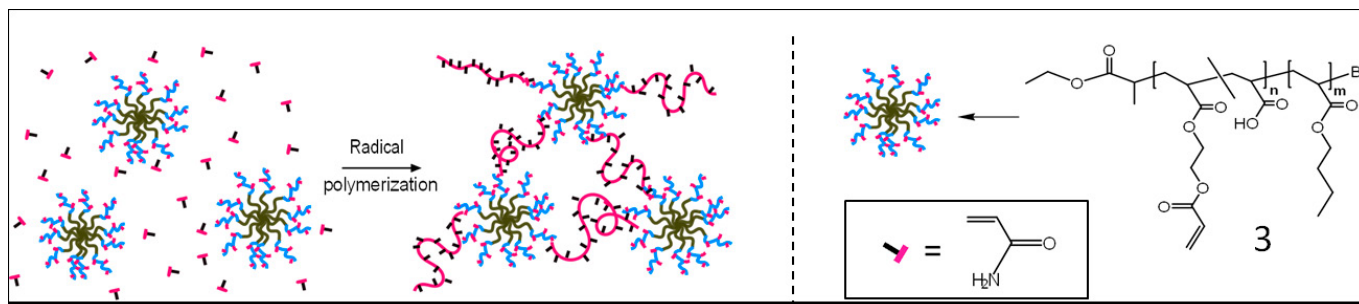13. Xiao, L.; Zhu, J.; Londono, D. J.; Pochan, D. J.; Jia, X. Soft Matter 2012, 8, (40), 10233-10237.

Figure 2. Synthesis and characterization of BCM-crosslinked, mechano-responsive hydrogels[12,13]. BCMs were assembled from (PAA-g-HEA)-b-PnBA (3) and hydrogels were prepared by radical polymerization of acrylamide in the presence of crosslinkable BCMs.

SIMS Analysis of Metals: Depth Resolution Issues and Use of Sample Rotation

By Fred A. Stevie, Senior Researcher, North Carolina State University

Secondary Ion Mass Spectrometry (SIMS) is a proven analytical technique for many applications because of high sensitivity and depth resolution. The ability to locate and quantify impurities as a function of depth with an analysis method that uses an ion beam to remove material by sputtering has been very important for surface analysis.

Depth resolution is dependent on uniform erosion of the sample during ion bombardment. It has been known for some time that analysis of even single crystal silicon using O2+ bombardment can lead to formation of ripples that not only degrade depth resolution but result in a change in sputtering rate that complicates depth axis calibration.[1,2]

Metals comprise two thirds of the elements and approximately 25% of the earth's mass. Metals have many critical applications that can be aided by surface analysis. However, this class of materials is particularly susceptible to non-uniform sputtering. Metals are typically polycrystalline which means they are composed of many small crystals or grains. They also have grain boundaries and may have multiple phases which result in an inhomogeneous sample. Each grain has its own crystal orientation and sputtering into the grains with an ion beam will strike some grains in an aligned direction and some not aligned. For an aligned grain, the ion beam will penetrate further into the sample. As a result, a higher proportion of the energy of the incident ion will be imparted deeper in the sample which results in a lower sputtering rate compared with a grain not aligned where more of the incident ion energy is provided to the surface atoms. There is a corollary effect which explains the contrast observed when a Focused Ion Beam (FIB) is used to image a metal surface.[3,4] The ions that strike aligned grains penetrate deeper and generate fewer secondary electrons. Ions that strike unaligned grains have shallower penetration and generate more secondary electrons and these grains appear brighter than aligned grains. Figure 1 shows an example of secondary electron imaging of a chromium coated steel wire under Ga+ bombardment in an FIB instrument.[4] The steel grains are clearly visible and the grain size difference with the smaller chromium atoms is evident.

The difference in sputtering rate between aligned and not aligned grains can be quite significant. The result is topography formation and Fig 2 illustrates the impact for a SIMS crater in a metal layer.[2] The rough crater bottom will significantly degrade depth resolution. For some materials, the non-uniformity can be on the order of a micrometer for a crater that is only a few micrometers deep. Significant ion bombardment induced roughness can be measured with Scanning Electron Microscopy (SEM). If the sample can be viewed optically during sputtering, significant roughening will cause the crater region to become dark because the light used to view the sample is scattered. Roughening on a smaller scale may require measurement with Atomic Force Microscopy (AFM).

Topography formation can often be reduced by varying the angle of incidence, the beam energy, or the bombarding species. However, a method that has proven to reduce topography formation during sputtering is sample rotation. Even though metal grains sputter at different rates for different orientations, rotation of the sample during sputtering presents continually varying angles of the grain to the beam and the result is a uniform crater bottom. Sample rotation was first demonstrated for Auger Electron Spectroscopy (AES).[5] Applications of sample rotation using SIMS were easiest to achieve for quadrupole instruments because the physical space in the analyzer and extraction region is not as confined as for magnetic sector instruments. Analysis of a 1μm thick aluminum film using sample rotation showed significant improvement in depth resolution for quadrupole[6] and magnetic sector instruments.[7] High speed rotation is not required and a rate on the order of 12 rev/min can be sufficient.

Numerous sample rotation examples can be found for SIMS analysis. An inter-laboratory study of a nickel/chromium multilayer structure with AES, XPS and SIMS analysis showed significant improvement in depth resolution with sample rotation.[8] A similar result was obtained for a GaAs/AlGaAs superlattice.[9] AFM measurements that correlate removal of topography with analysis improvement have, for example, been documented for polycrystalline silicon[10], low energy O2+ bombardment used for ultra-shallow

measurements[11], and a ZnTe/GaAs study where the roughening originated at the interface.[12]

A limited number of magnetic sector SIMS instruments have sample rotation capability, but SIMS instruments with Time of Flight analyzers (TOF-SIMS) have more open geometry than the magnetic sectors. The utility of sample rotation has been demonstrated on a TOF-SIMS instrument for cluster beams such as C60[13] and the effect investigated with molecular dynamics simulations.[14]

Analysis of metals using SIMS has some complicating factors, particularly as a result of topography formation during ion bombardment. However, the use of sample rotation has proved to be an effective method to improve the depth resolution for analysis of this class of materials.

Figure 1. FIB secondary electron image of chromium coated steel wire showing contrast due to grain orientation. From FEI website[4]

References

1. F. A. Stevie, P. M. Kahora, D. S. Simons, P. Chi, J. Vac. Sci. Technol. A6, 2390 (1988)

2. SIMS, R. G. Wilson, F. A. Stevie, C. W. Magee, Wiley, New York (1989) pp. 2.7-1, 4.1-15

3. L. A. Giannuzzi, F. A. Stevie, Introduction to Focused Ion Beams, Springer (2005) p. 45

4. http://www.fei.com/uploadedfiles/documents/content/2006_06_fib_overview_pb.pdf

5. A. Zalar, Thin Solid Films, 124, 223 (1985)

6. F. A. Stevie, J. L. Moore, Surf. Interface Anal. 18, 147 (1992)

7. D. E. Sykes, A. Chew, Surf. Interface Anal. 21, 231 (1994)

8. S. Hofmann, A. Zalar, E.-H. Cirlin, J. J. Vajo, H. J. Mathieu, P. Panjan. Surf. Interface Anal. 20, 621 (1993)

9. E.-H. Cirlin, J. J. Vajo, T. C. Hasenberg, R. J. Hauenstein, J. Vac. Sci. Technol. A8, 4101 (1990)

10. S. J. Guilfoyle, A. Chew, N. E. Moiswiwitsch, D. E. Sykes, M. Petty, J. Phys.: Condens. Matter 10, 1699 (1998)

11. R. Liu, A. T. S. Wee, Appl. Surf. Sci. 231-232, 653 (2004)

12. P. Konarski, M. Hautala, Vacuum 47, 1111 (1996)

13. P. Sjovall, D. Rading, S. Ray, L. Yang, A. G. Shard, J. Phys. Chem. B114, 769 (2010)

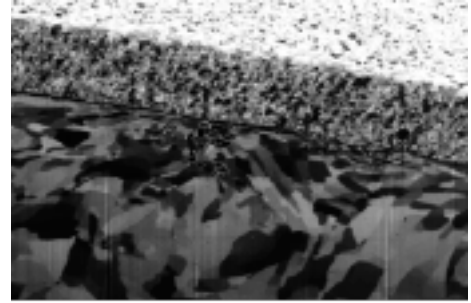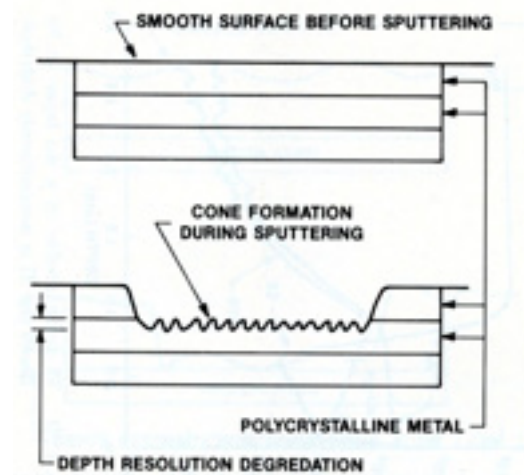14. B. J. Garrison, Z. Postawa, Chemical Physics Letters 506, 129 (2011)

Figure 2. Illustration of topography formation in SIMS crater. From Wilson, Stevie, Magee, 1989[2]

FDA Issues New Guidance Documents and Resolves to Issue Many More in 2013

By Phil Triolo, SurFACTS Regulatory Editor

The US FDA issued a few guidance documents just as 2012 ended, and has published a list of additional guidance documents it plans to issue in 2013.

Perhaps the most relevant of the recent trio of final guidance documents released on New Year's Eve is for electronic copies (eCopies) of medical device submissions.

eCopies are now required, not recommended, for 510(k)s, including third-party 510(k)s; De novo petitions; PMAs; PDPs; IDEs, except those for Compassionate or Emergency IDEs; HDEs; and Pre-Submission materials. eCopies are voluntary for MAFs, 513(g)s, and CLIA X Files.

(Sorry for the alphabet soup. Click here for a glossary.)

When required, at least one eCopy must accompany at least one paper copy of the signed cover letter and the complete paper submission in order for the submission to be accepted. The eCopy may be submitted on a compact disc, digital video disc, or flash drive. The eCopy must include all of the required information for FDA review, whereas the paper copy can include a placeholder cross-referencing the location of certain information in the eCopy. The cover letter must contain the eCopy statement described in Attachment 1 of the guidance and describe any differences between the paper version and the eCopy. The guidance outlines the format and naming requirements for the .pdf files that are to be submitted. The FDA offers a free "eSubmitter-eCopies" tool (which can be found by clicking here) at which it "strongly encourage[s] applicants to use."

The FDA will not accept any of the submissions that require eCopies that do not include at least one eCopy in the required format. Along the same lines, the final version of the FDA's guidance "Refuse to Accept Policy for 510(k)s," also issued on 31 December, explains the procedures and criteria FDA uses in "assessing whether a 510(k) submission meets a minimum threshold of acceptability and should be accepted for substantive review."

See here. That's pretty self explanatory. Assure that the "recommendations" of this guidance document are met, or you may find that you have to rewrite and resubmit your 510(k) and incur a significant delay in device clearance. Likewise, if submitting a PMA, assure that the recommendations of the 31-December-issued guidance "Acceptance and Filing Reviews for Premarket Approval Applications (PMAs)" are also addressed to minimize delays in processing your PMA.

By way of New Year's resolutions, the FDA published its list of the guidance documents it intends to issue in FY 2013. The list can be found here. The most anticipated of these, from the perspective of a medical device innovator, are the following final versions promised:

- Premarket Notification [510(k)] Submissions for Medical Devices that Include Antimicrobial Agents
- Investigational Device Exemptions (IDE) for Early Feasibility Medical Device Clinical Studies, Including Certain First in Human (FIH) Studies
- Design Considerations for Pivotal Clinical Investigations for Medical Devices
- De novo Classification Process (Evaluation of Automatic Class III Designation)
- The 510(k) Program: Evaluating Substantial Equivalence in Premarket Notifications
- The Pre-Submission Program and Meetings with FDA Staff
- Mobile Medical Applications
- In Vitro Companion Diagnostic Devices

Interestingly, it has been my experience that the FDA is, for the most part, following the recommendations in the draft guidance on Pre-Submission meetings. Yet, the provisions of the proposed revisions to the De novo guidance are not yet being implemented, even though the possibility of industry disapproval of the proposed revisions, which represent a marked improvement over the current procedures, is slim to non-existent.

The most significant change proposed in the Pre-Sub guidance is that the FDA will commit to providing a written response to Pre-Sub materials within 90 days of their submission. This represents an improvement over the current practice of providing the minutes of the non-binding meetings for FDA approval. The major proposed change to the de novo process is that a pre de novo submission (PDS) of materials can be provided for FDA assessment of suitability prior to submission of the 510(k). If the FDA finds the materials presented in the PDS suitable for review, the de novo petition and 510(k) could be submitted simultaneously with proposed reductions in overall review times.

May all your submissions be reviewed in record time in 2013!

Wanted: Members

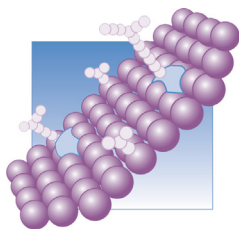## To be leaders in the surface science community

- Join a forum that fosters discussion and sharing of surface and interfacial information
- Have your voice heard and your interests represented within the surface science and biomedical community
- Help shape workshops and symposia that further the world-wide education of surface science
- Promote understanding of interfacial issues common to researchers, bio-medical engineers and material scientists.

Benefits of Membership:

- Discounted registration at BioInterface, the annual symposium of the Surfaces in Biomaterials Foundation.
- Your logo and a link to your Web site in the member directory on the official website of the Foundation, www.surfaces.org.
- Complimentary full page ad in SurFACTS, the Foundation's newsletter and discounts on all advertising.

Join the Foundation that connects the academic, industrial, and regulatory committees within the surface science/biomedical communities!

Visit the Foundation at www.surfaces.org for a membership application or call 651-290-6267.

Surfaces in **Biomaterials** Foundation

Thank You to Our Members!

APS — AMERICAN PRECLINICAL SERVICES

AST PRODUCTS, INC.

BASF — The Chemical Company

BAUSCH + LOMB

BIOCOAT INCORPORATED

CAL POLY

carmeda — A SUBSIDIARY OF W. L. GORE & ASSOCIATES

Corline

COVIDIEN

EAG — Evans Analytical Group

EnBio — Surface Enhancing Technologies

ExThera MEDICAL

GORE — Creative Technologies Worldwide

IonAtom Consulting, LLC

LIFECORE BIOMEDICAL

NESAC/BIO — Frontiers in Biomedical Surface Analysis

PLASMA TECHNOLOGY SYSTEMS

PVA TePla

Surface Solutions Laboratories

UCD DUBLIN

UNIVERSITY OF LOUISVILLE AND JEWISH HOSPITAL — CARDIOVASCULAR INNOVATION INSTITUTE